

# Color representation method using RGB color binary-weighted computer-generated holograms

Masato Fujiwara<sup>1</sup>, Naoki Takada<sup>2,\*</sup>, Hiromitsu Araki<sup>1</sup>, Shohei Ikawa<sup>3</sup>, Yuki Maeda<sup>1</sup>, Hiroaki Niwase<sup>1</sup>, Minoru Oikawa<sup>2</sup>, Takashi Kakue<sup>4</sup>, Tomoyoshi Shimobaba<sup>4</sup>, and Tomoyoshi Ito<sup>4</sup>

<sup>1</sup>Graduate School of Integrated Arts and Sciences, Kochi University, Kochi 780-8520, Japan

<sup>2</sup>Science Department, Natural Sciences Cluster, Research and Education Faculty, Kochi University, Kochi 780-8520, Japan

<sup>3</sup>Faculty of Science, Kochi University, Kochi 780-8520, Japan

<sup>4</sup>Graduate School of Engineering, Chiba University, Chiba 263-8522, Japan

\*Corresponding author: [ntakada@is.kochi-u.ac.jp](mailto:ntakada@is.kochi-u.ac.jp)

Received April 2, 2018; accepted June 25, 2018; posted online July 30, 2018

We propose a method for color electroholography using a simple red–green–blue (RGB) gradation representation method without controlling the respective brightness of the reference RGB-colored lights. The proposed method uses RGB multiple bit planes comprising RGB binary-weighted computer-generated holograms with various light transmittances. The object points of a given three-dimensional (3D) object are assigned to RGB multiple bit planes according to their RGB gradation levels. The RGB multiple bit planes are sequentially displayed in a time-division-multiplexed manner. Consequently, the proposed method yields a color gradation representation of a reconstructed 3D object.

OCIS codes: 090.1705, 090.1760, 090.2870.  
doi: 10.3788/COL201816.080901.

Holography<sup>[1]</sup> is an optical technology that can reliably record and reconstruct three-dimensional (3D) images. 3D images are digitally recorded on computer-generated holograms (CGHs) as an interference fringe obtained from light diffraction calculated by a computer. Electroholography using CGH is expected to enable the ultimate 3D television (3DTV), because it can reconstruct 3D movies using a spatial light modulator (SLM).

Color electroholography is indispensable for developing a 3DTV. Color electroholography using three SLMs for red–green–blue (RGB) lights has previously been reported<sup>[2–4]</sup>. Likewise, color electroholography using a single SLM has been investigated. Furthermore, the space-division method<sup>[5]</sup>, depth-division method<sup>[8,9]</sup>, and time-division method<sup>[10–14]</sup> have been proposed.

The study of gradation representation is very useful to yield high quality color representation of reconstructed 3D images using electroholography. A binary CGH can be used in an amplitude-modulation-type SLM, for example, a liquid-crystal display (LCD) panel and a digital micromirror device (DMD). However, the image quality of 3D objects reconstructed from binary CGH is deteriorated due to the error caused by converting holographic data to binary CGH. The gradation representation of the reconstructed 3D images from binary CGH is not easy. Gradation representation approaches using the direct-search method<sup>[15,16]</sup> and error-diffusion method<sup>[17,18]</sup> have been reported. The former is an iterative method. The gradation representation approach has also been used for the time-multiplexing technique with multiple bit planes obtained by controlling the intensity of the reference light<sup>[19]</sup>.

However, it is not easy for these approaches<sup>[15–19]</sup> to freely adjust the gradation of the reconstructed 3D object.

In our recent work, a gradation representation method using multiple bit planes composed of binary-weighted CGHs (BW-CGHs) has been proposed<sup>[20,21]</sup>, which provides high quality gradation representation to the respective electroholographies using LCD panels<sup>[20]</sup> and DMD<sup>[21]</sup>. In this work, we propose color electroholography using our gradation representation method. We used three transmissive LCD panels of a projector (Epson Corp. EMP-TW1000) as SLMs. A color image is input into the projector and divided into red, green, and blue images. The RGB images are displayed on the LCD panels for RGB reference lights, respectively.

Figure 1 shows the outline of the BW-CGH for green reference light. The BW-CGH shown in Fig. 1(b) is the improved binary CGH for the green reference light. In the conventional binary CGH shown in Fig. 1(a), we used a simple algorithm to obtain an in-inline

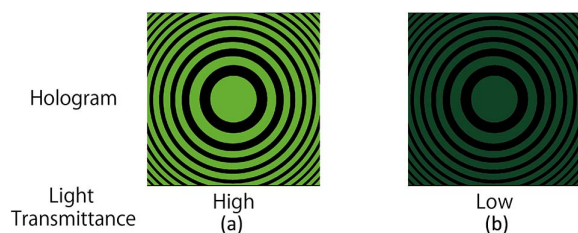


Fig. 1. (a) Conventional binary CGH and (b) BW-CGH for green reference light.

hologram from a 3D object expressed by a point cloud. The amplitude distribution of the hologram is given by the following equation<sup>[22]</sup>:

$$I(x_h, y_h, 0) = \sum_{i=1}^N A_i \cos \left\{ \frac{\pi}{\lambda z_i} [(x_h - x_i)^2 + (y_h - y_i)^2] \right\}, \quad (1)$$

where  $I(x_h, y_h, 0)$  is the amplitude distribution of the point  $(x_h, y_h, 0)$  on the hologram,  $(x_i, y_i, z_i)$  is the coordinate of the  $i$ th point on the 3D object,  $A_i$  is the intensity of the object point,  $N$  is the number of object points of the 3D model, and  $\lambda$  is the wavelength of the reference light. Equation (1) is obtained using the Fresnel approximation. After the calculation of Eq. (1), the conventional binary CGH is generated from the binarized amplitude distribution of the hologram by a threshold value of zero<sup>[23]</sup>. As shown in Fig. 1(a), the binary CGH is shown in black and green (bright). Black and green (bright) areas of the binary CGH show that the values of amplitude distribution of the hologram are less than and not less than zero, respectively.

The intensity of an object point  $A_i$  is set to 1.0 when the binary CGH for a BW-CGH is generated using Eq. (1). Figure 1(b) shows the BW-CGH generated by changing the brightest green color in the binary CGH [Fig. 1(a)] to the green color with one of various gradation levels. The light passing through the green color area of the BW-CGH [Fig. 1(b)] is weakened compared to the light passing through the brightest green color area of the binary CGH [Fig. 1(a)]. Therefore, the light transmittance of the BW-CGH [Fig. 1(b)] is less than that of the binary CGH [Fig. 1(a)].

Figure 2 shows the reconstructed object points from the BW-CGHs displayed on the SLM. Here, object point  $c$  is reconstructed from the conventional binary CGH, and object points  $a$  and  $b$  are reconstructed from the BW-CGHs drawing the green color with different gradation levels. The light intensity of object point  $c$  is the highest, whereas that of object point  $b$  is higher than that of object point  $a$ . Higher gradation levels of the green color on a BW-CGH result in higher light intensity of the reconstructed object point.

Figure 3 shows how to assign the respective object points with eight gradation levels to multiple bit planes

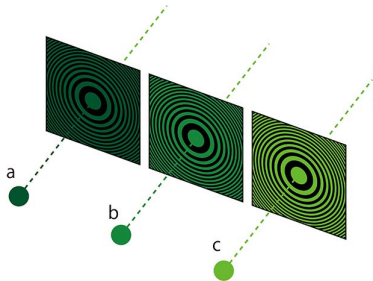


Fig. 2. Light intensities of the reconstructed object points from BW-CGHs shown in green with various gradation levels.

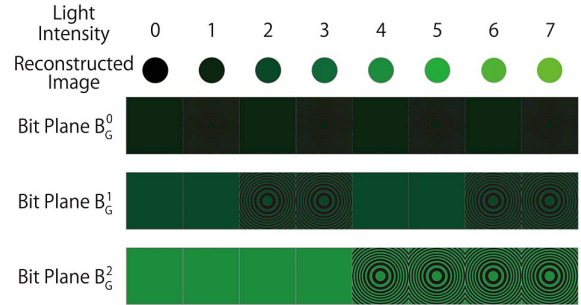


Fig. 3. Assignment of the object points of the 3D object to the bit planes comprising BW-CGHs with different gradation levels.

comprising the BW-CGHs. In Fig. 3, the eight object points with gradation levels ranging from 0 to 7 are assigned to the multiple green bit planes:  $B_G^0$ ,  $B_G^1$ , and  $B_G^2$ , respectively. The  $m$ th green bit plane is described by  $B_G^m$ , and the reconstructed object points from bit plane  $B_G^m$  have  $2^m$  gradation levels. Therefore, the reconstructed object points from the bit planes  $B_G^0$ ,  $B_G^1$ , and  $B_G^2$  have  $2^0$ ,  $2^1$ , and  $2^2$  gradation levels, respectively. For example, the object point with a gradation level of 5, which is equal to the sum of  $2^0$  and  $2^2$ , is assigned to the bit planes  $B_G^0$  and  $B_G^2$ . The green reference light illuminates the multiple bit planes  $B_G^0$ ,  $B_G^1$ , and  $B_G^2$ , which are repeatedly displayed on an LCD panel at a regular time interval  $\Delta t$ , and the 3D gradation image of the object point with gradation level is reconstructed. Here, the intensity of the green reference light is kept constant.

As shown in Fig. 4, the RGB object points with the gradation level of 5 are reconstructed from the RGB bit planes  $B^0$ ,  $B^1$ , and  $B^2$ , respectively. Herein, the RGB bit planes  $B^0$ ,  $B^1$ , and  $B^2$  are repeatedly displayed on the LCD panels corresponding to the RGB reference lights at a regular time interval  $\Delta t$ . The gray reconstructed object point with the gradation value of 5 is synthesized from the RGB reconstructed object points using the optical setup shown in Fig. 5. Herein, the input color image is synthesized in the  $m$ th RGB-colored bit plane  $B_{RGB}^m$  from the RGB bit planes  $B_R^m$ ,  $B_G^m$ ,  $B_B^m$ , as shown in Fig. 6. The RGB colors of the respective bit planes are expressed in 8 bit RGB data. Therefore, the synthesized  $m$ th

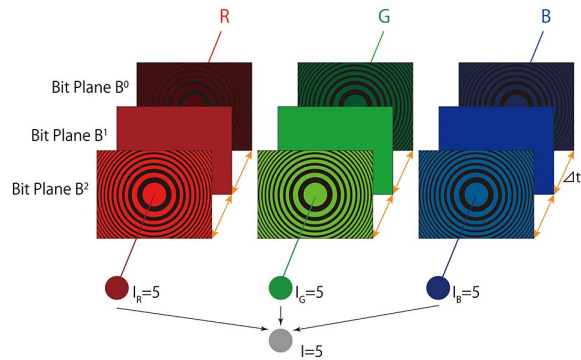


Fig. 4. Color reconstructed object point from RGB bit planes comprising BW-CGHs with different gradation levels.

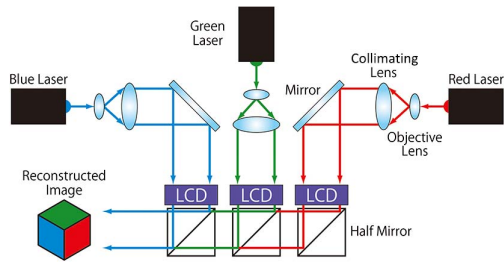


Fig. 5. Optical setup for color electroholography using RGB multiple bit planes comprising BW-CGHs.

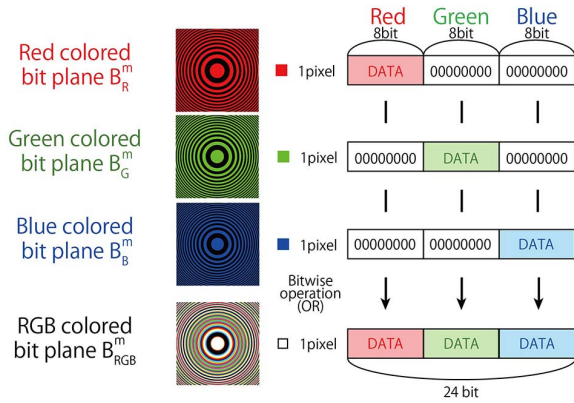


Fig. 6. RGB-colored bit plane  $B_{RGB}^m$  synthesized from RGB bit planes  $B_R^m$ ,  $B_G^m$ ,  $B_B^m$ .

RGB-colored bit plane  $B_{RGB}^m$  is expressed in 24 bit RGB-colored data. The frame rate is inversely proportional to the number of bit planes when the proposed method is adopted to a 3D movie.

We evaluated the proposed method using the optical setup shown in Fig. 5. We used three laser lights with wavelengths of 642, 532, and 473 nm as RGB reconstructing lights for color electroholography, respectively. Each laser light is converted into a parallel light by an objective lens and a collimating lens. The parallel light is made incident on each LCD panel. In Fig. 5, we used three LCD panels mounted on a projector (Epson Inc. EMP-TW1000, L3C07U series). The specifications of the LCD panels are as follows: pixel interval 8.5  $\mu\text{m}$ , resolution 1920  $\times$  1080, refresh rate 60 Hz, and size 16.4 mm  $\times$  9.2 mm. The projector is connected to a PC equipped with an Intel Core i7 3770 (clock speed: 3.4 GHz, quad-core) Linux (CentOS 6.4) as its operating system, the NVIDIA GeForce GTX TITAN as the graphics processing unit (GPU), the CUDA 5.0 software-development kit for the GPU programming, and Open Graphics Library (GL) as the graphics application programming interface (API). In Fig. 5, the mirrors are changed to dichroic mirrors.

In order to evaluate the proposed method, we used the original 3D model “Stanford bunny,” comprising 12,684 object points without hidden surfaces. Figures 7(b)–7(n)

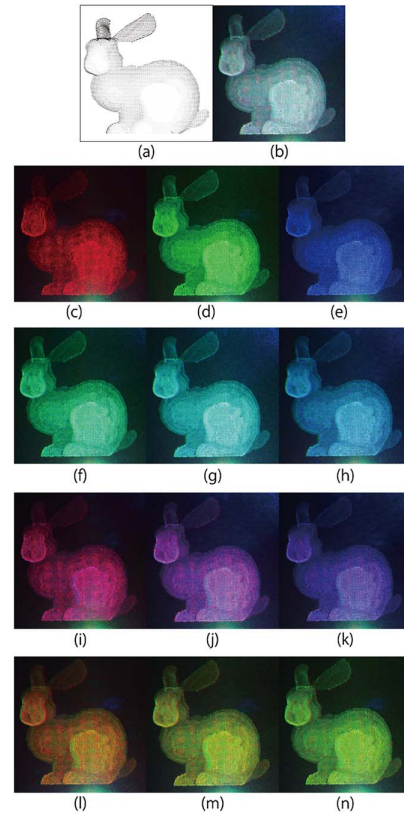


Fig. 7. Multicolored reconstructed real images using the proposed method. (a) The white 3D objects “Stanford bunny” with gradation. (b) The reconstructed real image from the white 3D objects “Stanford bunny.” (b)–(n) The multicolored reconstructed image.

show the multicolored reconstructed real images using the original 3D model “Stanford bunny.” Table 1 shows the gradation values of the RGB area of BW-CGHs used in the RGB bit planes:  $B_R^0$ ,  $B_R^1$ ,  $B_R^2$ ,  $B_G^0$ ,  $B_G^1$ ,  $B_G^2$ ,  $B_B^0$ ,  $B_B^1$ ,  $B_B^2$ . These gradation values were determined using the visual observation of the reconstructed real images from various gradation values because the gradation values of the colored area of BW-CGH can be easily changed.

Furthermore, we tried to reconstruct the seven-colored 3D object model. In Fig. 8, the seven-colored 3D object is divided into the red, green, and blue objects, and the object points of the divided respective colored objects assigned to the respective colored multiple bit planes  $B_R^0$ ,  $B_R^1$ ,  $B_R^2$ ,  $B_G^0$ ,  $B_G^1$ ,  $B_G^2$ ,  $B_B^0$ ,  $B_B^1$ , and  $B_B^2$  are shown. Figure 9 shows the seven-colored reconstructed real image. Herein, the gradation values of the RGB areas of the BW-CGHs used in RGB bit planes  $B_R^0$ ,  $B_R^1$ ,  $B_R^2$ ,  $B_G^0$ ,  $B_G^1$ ,  $B_G^2$ ,  $B_B^0$ ,  $B_B^1$ , and  $B_B^2$  were set to 100, 130, 200, 135, 165, 255, 135, 165, and 255, respectively. The reconstructed real image is composed of seven colors: red, green, blue, cyan, magenta, yellow, and white. The real image shown in Fig. 9 is reconstructed from three RGB multiple bit planes in a time-division-multiplexed manner. Therefore, the real image is displayed at a frame rate of 20 frame/s because the refresh rate of LCD panel is 60 Hz.



**Table 1.** Gradation Values of the Colored Area of BW-CGHs of Multiple Bit Planes

Figure	Gradation Values of Bit Planes								
	Red Bit Plane			Green Bit Plane			Blue Bit Plane		
	$B_R^0$	$B_R^1$	$B_R^2$	$B_G^0$	$B_G^1$	$B_G^2$	$B_B^0$	$B_B^1$	$B_B^2$
Fig. 7(b)	125	150	240	135	165	255	135	165	255
Fig. 7(c)	135	165	255	0	0	0	0	0	0
Fig. 7(d)	0	0	0	135	165	255	0	0	0
Fig. 7(e)	0	0	0	0	0	0	135	165	255
Fig. 7(f)	0	0	0	135	165	255	80	115	180
Fig. 7(g)	0	0	0	135	165	255	135	165	255
Fig. 7(h)	0	0	0	85	120	170	135	165	255
Fig. 7(i)	135	165	255	0	0	0	90	120	170
Fig. 7(j)	135	165	255	0	0	0	135	165	255
Fig. 7(k)	75	110	160	0	0	0	135	165	255
Fig. 7(l)	135	165	255	85	120	170	0	0	0
Fig. 7(m)	135	165	255	120	150	240	0	0	0
Fig. 7(n)	105	140	200	135	165	255	0	0	0

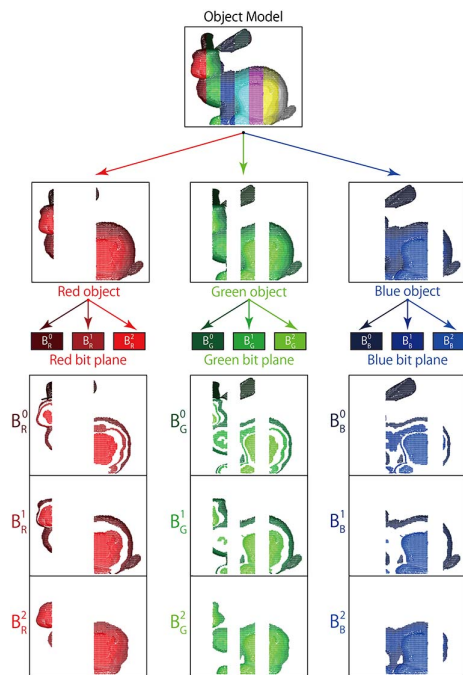


Fig. 8. Assignment of the object points of the seven-color 3D model to RGB multiple bit planes.

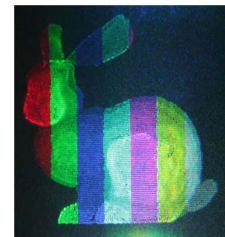


Fig. 9. Reconstructed real image of the seven-color 3D model.

reference light. We consider the proposed method to be useful for color adjustment of electroholography.

This work was partially supported by the Japan Society for the Promotion of Science through a Grant-in-Aid for Scientific Research (C) (No. 15K00153).

## References

1. D. Gabor, *Nature* **161**, 777 (1948).
2. F. Yaraş, H. Kang, and L. Onural, *Appl. Opt.* **48**, H48 (2009).
3. H. Nakayama, N. Takada, Y. Ichihashi, S. Awazu, T. Shimobaba, N. Masuda, and T. Ito, *Appl. Opt.* **49**, 5993 (2010).
4. J. Roh, K. Kim, E. Moon, S. Kim, B. Yang, J. Hahn, and H. Kim, *Opt. Express* **25**, 14774 (2017).
5. H. Sato, T. Kakue, Y. Ichihashi, Y. Endo, K. Wakunami, R. Oi, K. Yamamoto, H. Nakayama, T. Shimobaba, and T. Ito, *Sci. Rep.* **8**, 1500 (2018).
6. S. Yamada, T. Kakue, T. Shimobaba, and T. Ito, *Sci. Rep.* **8**, 2010 (2018).
7. T. Ito, T. Shimobaba, H. Godo, and M. Horiuchi, *Opt. Lett.* **27**, 1406 (2002).

8. M. Makowski, M. Sypek, and A. Kolodziejczyk, *Opt. Express* **16**, 11618 (2008).
9. M. Makowski, M. Sypek, I. Ducin, A. Fajst, A. Siemion, J. Suszek, and A. Kolodziejczyk, *Opt. Express* **17**, 20840 (2009).
10. T. Shimobaba and T. Ito, *Opt. Rev.* **10**, 339 (2003).
11. M. Oikawa, T. Shimobaba, T. Yoda, H. Nakayama, A. Shiraki, N. Masuda, and T. Ito, *Opt. Express* **19**, 12008 (2011).
12. H. Sasaki, K. Yamamoto, K. Wakunami, Y. Ichihashi, R. Oi, and T. Senoh, *Sci. Rep.* **4**, 1 (2014).
13. H. Araki, N. Takada, H. Niwase, S. Ikawa, M. Fujiwara, H. Nakayama, T. Kakue, T. Shimobaba, and T. Ito, *Appl. Opt.* **54**, 10029 (2015).
14. H. Araki, N. Takada, S. Ikawa, H. Niwase, Y. Maeda, M. Fujiwara, H. Nakayama, M. Oikawa, T. Kakue, T. Shimobaba, and T. Ito, *Chin. Opt. Lett.* **15**, 120902 (2017).
15. M. Clark, *Appl. Opt.* **38**, 5331 (1999).
16. T. Leportier, M. C. Park, Y. S. Kim, and T. Kim, *Opt. Express* **23**, 3403 (2015).
17. F. Fetthauer, S. Weissbach, and O. Bryngdahl, *Opt. Commun.* **114**, 230 (1995).
18. Y. Matsumoto and Y. Takaki, *Opt. Lett.* **39**, 3433 (2014).
19. Y. Takaki and M. Yokouchi, *Opt. Express* **19**, 7567 (2011).
20. M. Fujiwara, N. Takada, H. Araki, S. Ikawa, H. Niwase, Y. Maeda, H. Nakayama, T. Kakue, T. Shimobaba, and T. Ito, *Opt. Eng.* **56**, 023105 (2017).
21. M. Fujiwara, N. Takada, H. Araki, C. W. Ooi, S. Ikawa, Y. Maeda, H. Niwase, T. Kakue, T. Shimobaba, and T. Ito, *Chin. Opt. Lett.* **15**, 060901 (2017).
22. N. Masuda, T. Ito, T. Tanaka, A. Shiraki, and T. Sugie, *Opt. Express* **14**, 603 (2006).
23. W.-H. Lee, *Appl. Opt.* **18**, 3661 (1979).